Sensors and Materials, Vol. 29, No. 5 (2017) 545–553
MYU Tokyo

S & M 1348

Nonenzymatic Nitrogen-Doped Carbon Nanofiber-Supported NiO_x Glucose Sensor

Khaled A. Elsayed, Ahmed A. Elzatahry,[1] Ruqaiah Nasser,[1]
K. A. Khalil,[2,3] Tarek S. Kayed, and Aboubakr M. Abdullah[4*]

Department of Basic Sciences and Humanities, College of Engineering,
University of Dammam, Dammam, Kingdom of Saudi Arabia
[1]Materials Science and Technology Program, College of Arts and Sciences,
Qatar University, P.O. Box 2713, Doha, Qatar
[2]Mechanical Engineering Department, King Saud University,
P.O. Box 800, Riyadh 11421, Kingdom of Saudi Arabia
[3]Materials Engineering and Design Department, South Valley University, Aswan, Egypt
[4]Center for Advanced Materials, Qatar University, P.O. Box 2713, Doha, Qatar

(Received August 23, 2016; accepted December 5, 2016)

Keywords: glucose nonenzymatic sensor, carbon nanofiber, nickel oxide

The glucose electrooxidation reaction at NiO_x nanoparticles loaded on a nitrogen-doped carbon nanofiber (N-CNF)-modified glassy carbon electrode (NiO_x@N-CNF/GCE) in an alkaline medium was studied. The N-CNF was produced by an electrospinning technique to acquire a large surface area. The produced electrode was characterized by X-ray diffraction (XRD) and scanning electron microscopy (SEM) coupled with energy-dispersive X-ray (EDX) analysis. The electrocatalytic properties of this electrode towards glucose oxidation were tested by cyclic voltammetry and linear sweep voltammetry (LSV). The NiO_x@N-CNF/GCE catalytic activity towards glucose oxidation in an alkaline medium was found to be excellent in terms of measured glucose concentration and electrode stability. It showed high reproducibility and stability towards glucose oxidation with activity retention even after 100 cycles of continuous potential scanning. In addition, NiO_x@N-CNF/GCE showed a good linear behavior of glucose concentration detection in the concentration range between 0.0 and 10.0 mM, which highlights its ability to be used as a nonenzymatic glucose biosensor.

1. Introduction

Glucose electrooxidation reaction has attracted research attention recently owing to its importance in many beneficial applications such as fuel cells (FCs) and nonenzymatic sensors.[1–3] Many research efforts are currently focused on developing efficient biosensors for glucose nonenzymatic direct oxidation. Initially, precious metals, e.g., Au and Pt, were considered the main catalysts for the electrocatalytic oxidation of glucose in an alkaline medium because of their low oxidation potential as well as high current densities.[4–7] However, these electrodes suffer from carbonaceous poisoning during the oxidation process, which results in the blocking of the active site available for the reaction.[4–7] Recently, research has been devoted to using nonprecious transition metal oxides such as NiO_x, CoO_x, and MnO_x as alternative catalysts for glucose oxidation in an alkaline

*Corresponding author: e-mail: bakr@qu.edu.qa, abubakr_2@yahoo.com
http://dx.doi.org/10.18494/SAM.2017.1452

ISSN 0914-4935

medium[1–3,8,9] Among the aforementioned transition metal oxides, NiO_x is considered one of the most promising catalysts for glucose oxidation owing to its extremely high activity and stability as well as easy preparation in many structures.[1,3]

Although tremendous effort has been devoted to replacing the conventional carbon black support materials in many electrochemical technologies, e.g., polymer electrolyte membrane fuel cells (PEMFCs) and supercapacitors with large-surface-area carbon materials such as reduced graphene oxide, CNFs, and carbon nanotubes,[1,2,9–13] few studies were focused on the use of CNFs for nonenzymatic glucose electrooxidation.[14] In this regard, N-CNFs are produced from affordable nitrogen-containing polymeric materials with high molecular weights by electrospinning techniques followed by graphitization. As N-CNFs have an enormous tendency to conduct electricity, they can be used as a support for loading different metal oxide nanoparticles (electrocatalysts)[10–13] for the electrocatalysis of different reactions. In addition, using N-CNFs, which have a large surface area, enhances the dispersion and prevents the aggregation of the deposited metal oxide nanoparticles, as well as improves both the stability and electrocatalytic activity of such nanoparticles.[10–13]

Although few researchers studied NiO_x/CNF electrodes as nonenzymatic sensors for glucose,[14–19] in this work, a nitrogen-doped carbon nanofiber (N-CNF) that is loaded with NiO_x nanoparticles on a glassy carbon electrode (NiO_x@N-CNF/GCE) was investigated. The electrocatalytic activity of the prepared electrode was investigated as a nonprecious and nonenzymatic glucose oxidation electrocatalytic activity in an alkaline medium. The NiO_x@N-CNF was prepared by mixing a nickel nitrate solution with an N-CNF followed by calcination in argon atmosphere. The prepared electocatalyst was characterized by cyclic voltammetry, linear sweep voltammetry (LSV), X-ray diffraction (XRD), and scanning electron microscopy (SEM) coupled with energy-dispersive X-ray (EDX) analysis for the mapping of the electrode surface in addition to Brunauer–Emmett–Teller (BET) analysis for surface area measurements.

2. Experimental Methods

All chemicals used in this study were of analytical grade and purchased from Sigma-Aldrich. The deionized water from a Milli-Q water purification system with a resistivity of 18.6 MΩ was used to prepare all aqueous solutions. The NiO_x@N-CNF has been produced recently according to methods developed by our research team.[11,12] Briefly, 10 g of polyacryonitrile (PAN) was dissolved in 100 mL of dimethyl dimethylformamide (DMF) at room temperature and the mixture was stirred to form a uniform precursor suspension. The uniform suspension was then introduced into the electrospinning apparatus shown in Fig. 1 to produce the proposed PAN fibers at a potential of 20 kV at a distance of 15 cm between the needle and the collector drum with a flow rate of 0.5 mL h^{-1}.

The nanofiber was then dried at 50 °C under vacuum and stabilized at 270 °C in air for 2 h. N-CNFs were then prepared by the carbonization of the CNFs by heat treatment at 800 °C for 5 h in high-purity nitrogen atmosphere.[11,12] The stabilization step was carried out to form a ladder-shaped structure that can handle elevated temperatures during the carbonization process.

To achieve 10 wt% loading of nickel oxide on N-CNFs, appropriate amounts of $Ni(NO_3)_2{\cdot}6H_2O$ and CNFs were mixed in deionized water. The solution pH was adjusted to 8 using a 1 M NaOH solution, and the mixture was stirred continuously for 3 h. The resulting material was filtered, rinsed several times with deionized water, and dried overnight in an oven at 80 °C, then calcined

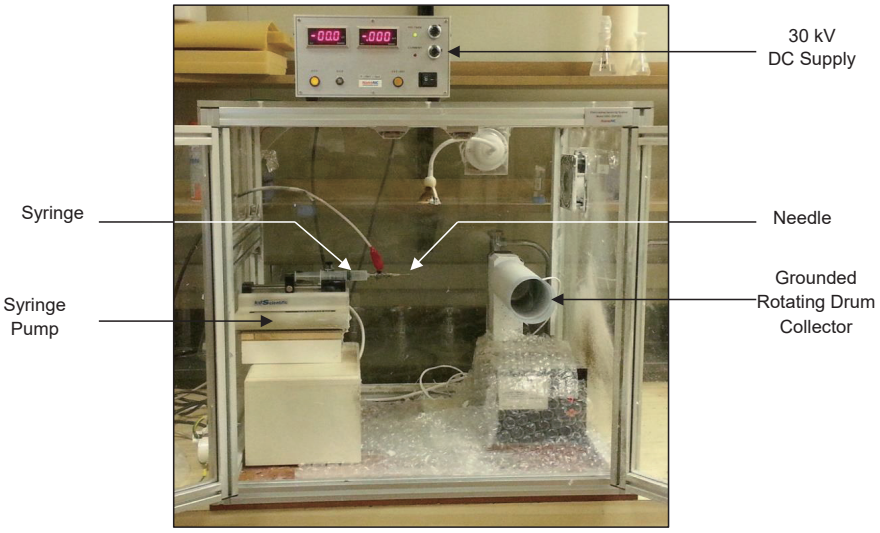

Fig. 1. (Color online) Electrospinning equipment used to prepare polymeric fibers.

at 400 °C for 2 h.[11,12] Note that, in contrast to what was performed in this work, Liu *et al.* electrospun Ni acetate with the PAN rather than loading after the carbonization process.[14]

The electrode was prepared by dispersing 4 mg of a NiO_x@N-CNF in 1% Nafion (diluted from 5% Nafion using isopropanol) with the aid of a sonicator for 2 h. Then, 5 µl of the prepared ink was cast on a GCE with an apparent surface area of 0.071 cm^2 and left to dry for 1 h.[11,12] All electrochemical measurements were performed using a Gamry potentiostat and a Pyrex 50 mL electrochemical cell using a saturated calomel electrode (SCE) as a reference electrode and a Pt wire as a counter electrode. The working electrode was the NiO_x@N-CNF/GCE. Electrochemical characterizations included cyclic voltametry and LSV in N_2-deaerated 0.5 M NaOH solutions with different glucose concentrations ranging from 0 to 20 mM.

A JSM-7100 F thermal field-emission SEM (FE-SEM) system was used to document the morphology of the as-prepared NiO_x@N-CNF. This system was equipped with an EDX spectrometer unit to map the surface of the electrode.

A Bruker D8 Advance X-ray diffractometer with Cu Kα radiation was used to identify the crystal structure and measure the average particle size. Furthermore, the surface area of the produced N-CNF was evaluated via H_2 adsorption/desorption, which was determined over the pressure range of 0–25 bar at ambient and liquid N_2 (77 K) using a Quantachrome Autosorb-1 system.

3. Results and Discussion

Figure 2 shows a SEM micrograph of electrospun PAN nanofibers obtained after preparation and before calcination. The nanofibers were distributed randomly. The nanofiber lengths ranging from few hundreds of nanometers to several micrometers were distributed normally. In addition, the nanofiber diameters were around 100 nm. The nanofibers were straight and their surface was smooth as can be seen in the same micrographs. The nanofibers were then stabilized in air for 2 h at 270 °C followed by carbonization at 800 °C for 5 h.

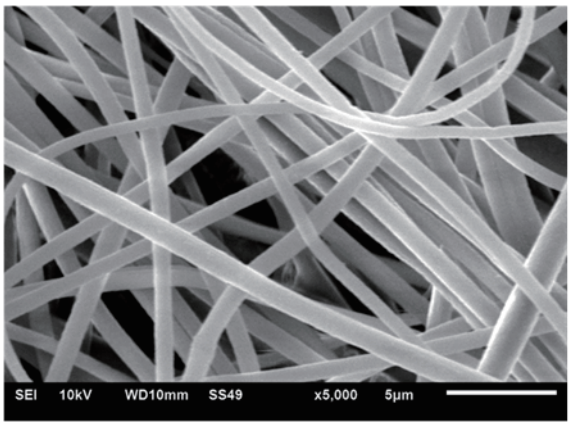

Fig. 2. SEM micrograph of the PAN nanofibers before calcination.

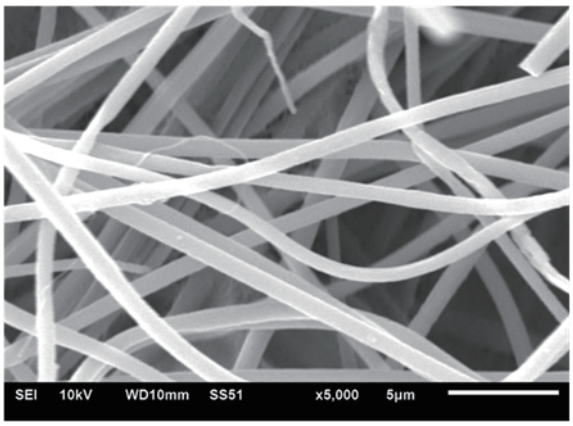

Fig. 3. SEM micrograph of N-CNF after calcination at 800 °C.

Figure 3 shows a SEM micrograph of the N-CNF after carbonization. The carbon content was increased to 90 wt% or higher as shown by EDX analysis as carbon fiber filaments were formed. The increase in carbon content was due to the evolution of many gases, e.g., N_2, and HCN.

After stabilization and carbonization, NiO_x was loaded and a calcination process was run at 400 °C for 2 h. This calcination process was designed to increase the nanoparticles' crystallinity in order to enhance the composite's electrocatalytic activity towards glucose oxidation.

Figure 4 shows the NiO_x nanoparticles before and after being loaded on the N-CNF and calcined at 400 °C. The TEM and SEM images show that the particles exist in clusters of 100 nm size with particles of 10 nm each, which have a cubic shape structure. Note that a parallel study was conducted and that the shape of the NiO_x nanoparticles and the calcination temperature were determined to affect the electrocatalytic properties significantly.

Figure 5 shows the XRD pattern of the N-CNF. The primary equatorial peak at 2θ = 16.8° corresponds to a d-spacing of 5.25 Å, while the second reflection at 2θ = 29.5° corresponds to a d-spacing of 3.05 Å. The peaks at 29.5 and 44° for the CNFs (carbonized at 800 °C) indicate (002) and (101) layers of hexagonal structures of graphite, respectively.[11,20]

The surface area measurements proved that the surface area of the N-CNF was reduced from 378 to almost 90 m^2g^{-1} after loading it with NiO_x. The reason for this might be the preferential deposition at the pores' edges.

Cyclic voltammograms (CVs) were taken in the absence and presence of glucose in an alkaline medium to study the glucose oxidation reaction at the as-prepared NiO_x@N-CNF/GCE. Figure 6 shows CVs of the NiO_x@N-CNF/GCE in the absence of glucose (curve a) and the presence of 20 mM glucose in 0.5 M NaOH (b) at a scan rate of 100 mV s^{-1}. The CV of the NiO_x@N-CNF in the absence of glucose (a) reveals the well-defined redox waves of Ni(II)/Ni(III) transformation in an alkaline medium at around 0.4 V, which leads to the formation of NiOOH[3,21] according to

$$Ni(OH)_2 + OH^- \leftrightarrow NiOOH + H_2O + e^-. \quad (1)$$

From the Ni 2p region (Fig. 7), it can be seen clearly that the oxidation state of nickel is +2 of type $Ni(OH)_2$.[22] The Ni $2p_{1/2}$ and Ni $2p_{3/2}$ spin-orbit coupling appears at 874.21 and 856.57 eV,

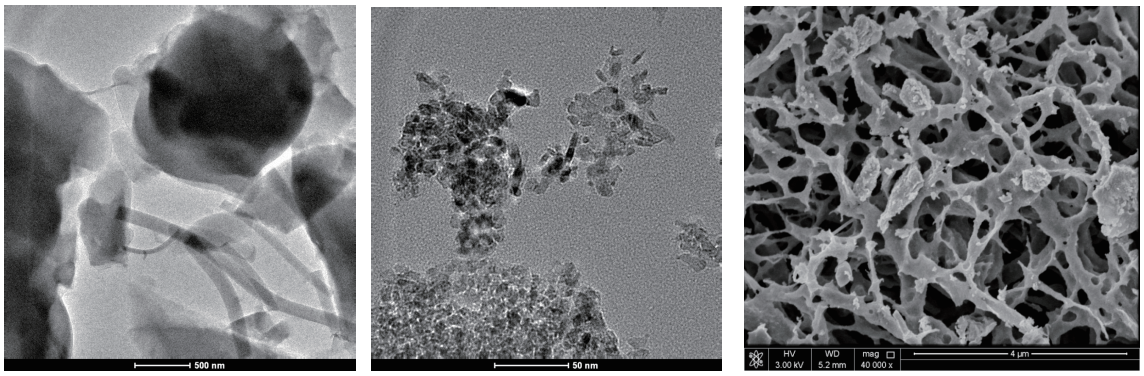

(a) (b) (c)

Fig. 4. SEM micrographs of NiO_x@N-CNF.

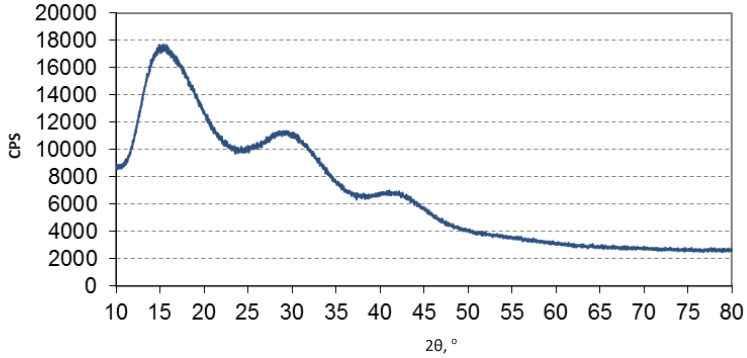

Fig. 5. (Color online) XRD scanning of N-CNF after calcination.

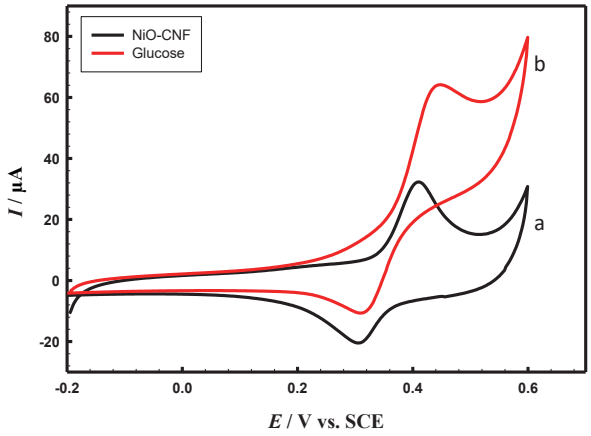

Fig. 6. (Color online) CVs of NiO_x@N-CNF/GCE in 0.5 M NaOH without (a, black) and with (b, red) 20 mM glucose at scan rate of 100 mV s^{-1}.

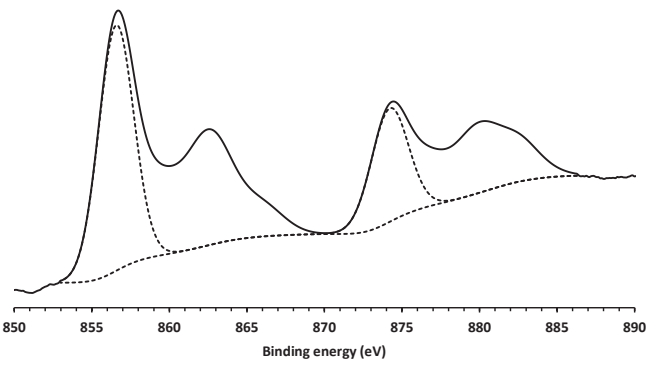

Fig. 7. High-resolution XPS spectrum of Ni 2p region.

respectively, of 17.64 eV spacing. The other spectral lines in the Ni region are due shake-up lines associated with Ni. In the presence of glucose (curve b), a notable increase in current and a well-defined peak for glucose oxidation were obtained.[3,20] According to the literature, it was reported

that the adsorbed glucose molecules undergo oxidation at the electrode surface at a potential that coincides with the transformation of Ni^{2+}/Ni^{3+}. This results in a reduction in the number of glucose adsorption active sites, whose overall rate tends to decrease, in addition to the poisoning effect of the products and/or intermediates of the glucose oxidation reaction.[3,23] This explains why, in the forward scan, the anodic current passes through a maximum. Note that the glucose electrocatalytic oxidation reaction occurs during the scan in the forward (less noble to more noble) direction as well as during the backward one. The glucose oxidation reaction occurs in the backward scan but without the same extent as that in the forwarded one, where a small reduction peak was observed during the scan in the more-to-less noble direction. The latter is attributed to the reduction of the remaining NiOOH.[3,20,21] Hence, the mechanism of GLO at the NiO_x@N-CNF/GC electrode can be described as[3,20,21]

$$Ni^{2+} \leftrightarrow Ni^{3+} + e^{-}, \tag{2}$$

$$Ni^{3+} + \text{glucose} \leftrightarrow Ni^{2+} + \text{products}. \tag{3}$$

Figure 8(a) shows the effect of scan rate on the CVs of the NiO@N-CNF/GCE in 0.5 M NaOH. Note that gradual increases in both anodic and cathodic peak currents were measured as the potential scan rate increased. Moreover, Fig. 8(b) shows the variation in peak current (I) with the scan rate (υ). A linear relationship between the peak current and the scan rate was obtained, indicating that the transformation process is a surface redox reaction.[3]

On the other hand, Fig. 9 presents the CVs of the NiO_x@N-CNF/GCE in 0.5 M NaOH containing 20 mM glucose at various scan rates ranging from 10 to 500 mV s^{-1}. Note that the potentials of the oxidation peaks shifted towards more positive values with increasing scan rate, and that the peak current of glucose oxidation increased gradually. A linear relationship was found between the current of the oxidation peak and the square root of the scan rate, which confirms a diffusion-controlled process for the glucose electrochemical redox reaction at the electrode surface.[3]

The stability of the prepared electrodes towards the proposed reaction, which is an important issue, was explored. Figure 10 shows the repetitive CVs (black is cycle # 1, red is cycle # 50, and

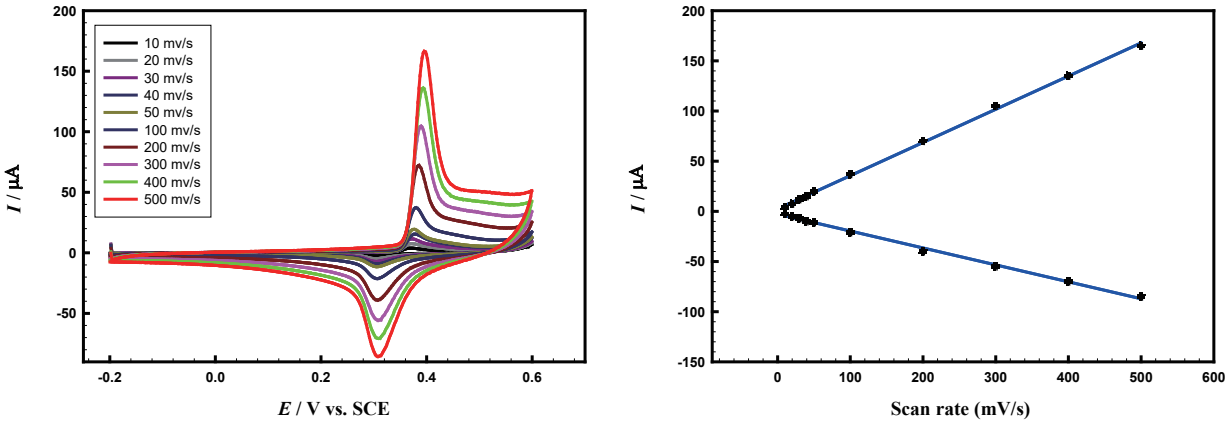

(a) (b)

Fig. 8. (Color online) (a) Effect of scan rate on the CVs of NiO_x@N-CNF/GCE electrode in 0.5 M NaOH and (b) anodic and cathodic current peaks of the NiO_x vs scan rate.

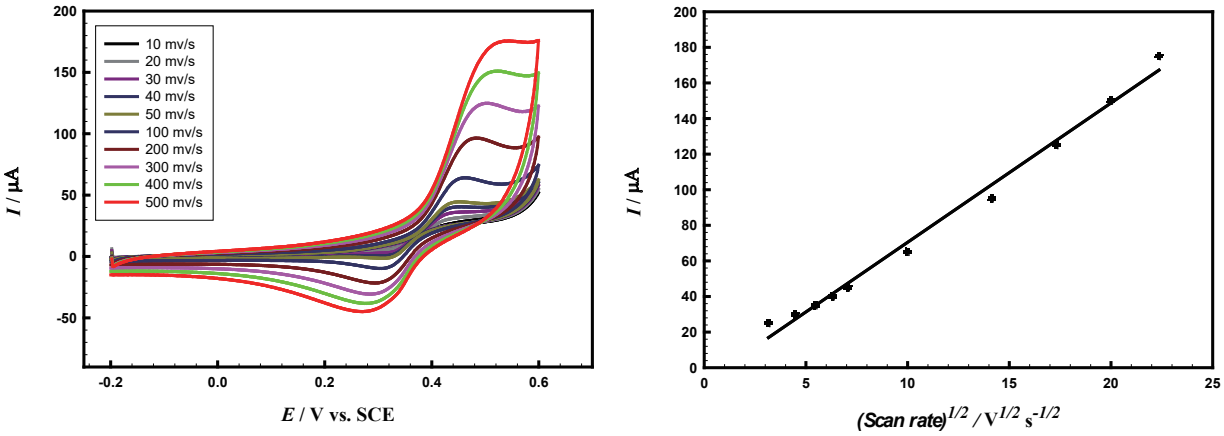

(a) (b)

Fig. 9. (Color online) (a) CVs of NiO_x@N-CNF/GCE at different scan rates in 0.5 M NaOH containing 20 mM glucose and (b) relationship between square root of scan rate and the anodic peak current, where data were taken from Fig. 9(a).

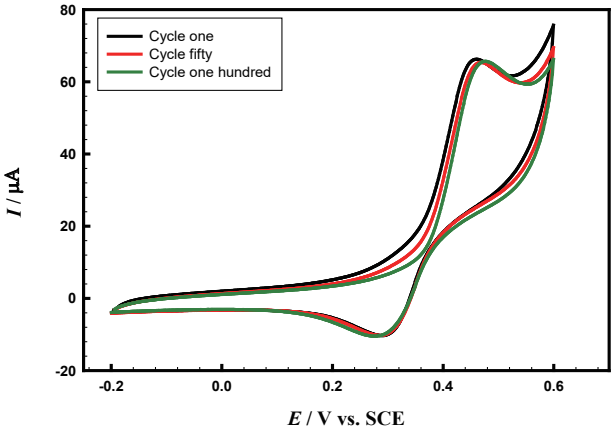

Fig. 10. (Color online) Repetitive CVs (black is cycle # 1, red is cycle # 50, and green is cycle # 100) of the NiO_x@N-CNF/GCE in 0.5 M NaOH containing 20 mM glucose at a scan rate of 100 mV s^{-1}.

green is cycle # 100) of the NiO_x@N-CNF/GCE in 0.5 M NaOH containing 20 mM glucose at a scan rate of 100 mV s^{-1}. The NiO_x@N-CNF/GCE electrode showed an extremely high stability with continuous cycling without current fading even at the cycle 100. However, a notable positive shift in onset potential was observed, which may be attributed to the diminishing of the β-NiOOH phase (the active phase for glucose oxidation in an alkaline medium) with repetitive cycling.[3]

3.1 Detection of glucose at NiO_x@CNF/GCE

The calibration curve for glucose detection in 0.5 M NaOH at the NiO_x@N-CNF/GCE was performed by LSV. Figure 11 shows the LSV responses of standard additions of 50 μl of 0.5 M glucose to 50 ml of 0.5 M NaOH. The peak current of glucose increased linearly with the

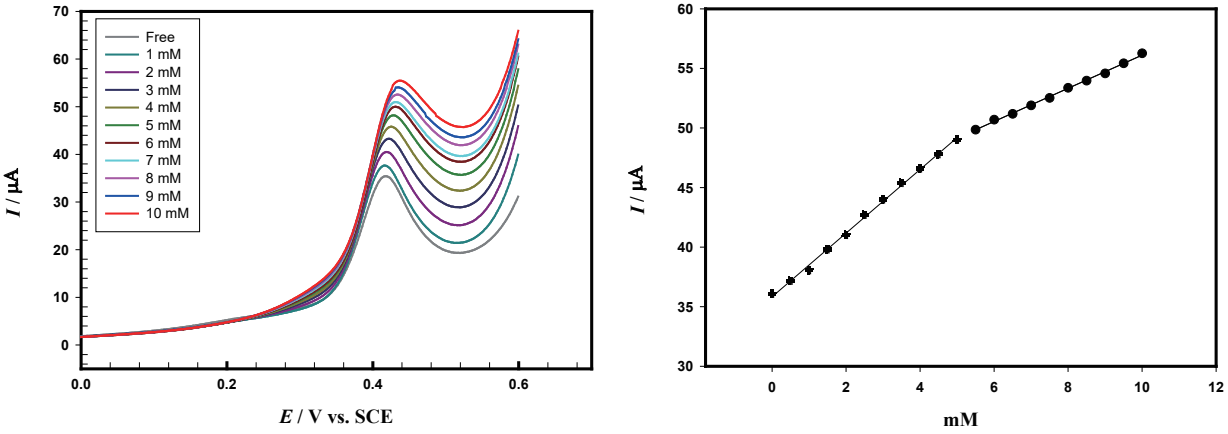

(a) (b)

Fig. 11. (Color online) (a) CVs of NiO_x@N-CNF/GCE at different concentrations of glucose in 0.5 M NaOH and (b) relation between glucose concentration and anodic peak current, where data were taken from Fig. 11(a).

incremental concentration of glucose in the range from 0.0 to 10.0 mM. The linear relationship between glucose concentration and the anodic peak current values of glucose oxidation can be described [Fig. 11(b)] with the linear regression equation I_p (µA) = 35.83 + 0.997C (mM) in the linear range of 0.5 to 5 mM with the correlation coefficient (r^2) = 0.9978, and with the regression equation I_p (µA) = 42.18 + 1.392C (mM) in the linear range of 5.5 to 10 mM with the correlation coefficient (r^2) = 0.9977.[6] Note that the electrode performance was very reproducible regardless of the glucose concentration, which makes this electrode very suitable for real applications.

4. Conclusions

A simple method for the fabrication of a NiO_x@N-CNF electrocatalyst was introduced. The prepared NiO_x@N-CNF/GCE electrode showed a good catalytic activity and high stability towards glucose electrooxidation in an alkaline medium. In addition, the NiO@N-CNF/GCE revealed potential to be used as a nonenzymatic glucose sensor in an alkaline medium in the analyte concentration range of 0.1–10 mM.

Acknowledgments

This work was funded by the Deanship of Scientific Research at the University of Dammam in Saudi Arabia under project number 2014145.

References

1 S. Fu, G. Fan, L. Yang, and F. Li: Electrochim. Acta **152** (2015) 146.
2 B. Yuan, C. Xu, L. Liu, Q. Zhang, S. Ji, L. Pi, D. Zhang, and Q. Huo: Electrochim. Acta **104** (2013) 78.
3 M. Jafarian, F. Forouzandeh, I. Danaee, F. Gobal, and M. G. Mahjani: J. Solid State Electrochem. **13** (2009) 1171.

4 B. Singh, F. Laffir, T. McCormac, and E. Dempsey: Sens. Actuators, B **150** (2010) 80.
5 D. Rathod, C. Dickinson, D. Egan, and E. Dempsey: Sens. Actuators, B **143** (2010) 547.
6 E. H. El-Ads, A. Galal, and N. F. Atta: J. Electroanal. Chem. **749** (2015) 42.
7 S. B. Aoun, G. S. Bang, T. Koga, Y. Nonaka, T. Sotomura, and I. Taniguchi: Electrochem. Commun. **5** (2003) 317.
8 M. R. Mahmoudian, W. J. Basirun, P. M. Woi, M. Sookhakian, R. Yousefi, H. Ghadimi, and Y. Alias: Mater. Sci. Eng. C, **59** (2016) 500.
9 Y. Wang, S. Zhang, W. Bai, and J. Zheng: Talanta **149** (2016) 211.
10 Y. Zhao, X. Bo, and L. Guo: Electrochim. Acta **176** (2015) 1272.
11 A. M. Al-Enizi, A. A. Elzatahry, A. M. Abdullah, M. A. AlMaadeed, J. Wang, D. Zhao, and S. Al-Deyab: Carbon **71** (2014) 276.
12 A. M. Al-Enizi, A. A. El-Zatahry, A. M. Abdullah, and S. S. Al-Deyab: ECS Trans. **61** (2014) 1.
13 A. M. Al-Enizi, M. A. Ghanem, A. A. El-Zatahry, and S. S. Al-Deyab: Electrochim. Acta **137** (2014) 774.
14 Y. Liu, H. Teng, H. Hou, and T. You: Biosens. Bioelectron. **24** (2009) 3329.
15 R. Ramasamy, K. Ramachandran, G. G. Philip, R. Ramachandran, H. A. Therese, and G. G. Kumar: RSC Adv. **5** (2015) 76538.
16 H.-Y. Shi, Y. Wu, W. Wang, W.-B. Song, and T.-M. Liu: Chem. Res. Chin. Univ. **29** (2013) 861.
17 W. Wang, Z. Li, W. Zheng, B. Dong, S. Li, and C. Wang: J. Nanosci. Nanotechnol. **10** (2010) 7537.
18 J. Zhang and X. Zhu: Peop. Rep. China, Patent No. CN103424446 A (2013) .
19 Y. Zhang, Y. Wang, J. Jia, and J. Wang: Sens. Actuators, B **171**–**172** (2012) 580.
20 V. S. Babu and M. S. Seehra: Carbon **34** (1996) 1259.
21 S. M. El-Refaei, M. M. Saleh, and M. I. Awad: J. Power Sources **223** (2013) 125.
22 M. C. Biesinger, B. P. Payne, L. M. Lau, A. Gersonb, and R. S. C. Smartb: Surf. Int. Anal. **41** (2009) 324.
23 S. M. El-Refaei, G. A. El-Nagar, A. M. Mohammad, and B. E. El-Anadouli: Progress in Clean Energy, Volume 1: Analysis and Modeling, eds. I. Dincer, C. O. Colpan, O. Kizilkan, and M. A. Ezan (Springer International Publishing, Cham, 2015) pp. 595–604.